Alzheimer's & Dementia: Diagnosis, Assessment & Disease Monitoring 10 (2018) 278-284

Special Section: State of the Field: Advances in Neuroimaging from the 2017 Alzheimer's Imaging Consortium

Regional tract-specific white matter hyperintensities are associated with patterns of aging-related brain atrophy via vascular risk factors, but also independently

Mohamad Habes[a,b,*], Guray Erus[a], Jon B. Toledo[c], Nick Bryan[a], Deborah Janowitz[d], Jimit Doshi[a], Henry Völzke[e], Ulf Schminke[f], Wolfgang Hoffmann[e,g], Hans J. Grabe[d,g], David A. Wolk[b], Christos Davatzikos[a]

[a]Center for Biomedical Image Computing and Analytics, University of Pennsylvania, Philadelphia, PA, USA
[b]Department of Neurology and Penn Memory Center, University of Pennsylvania, Philadelphia, PA, USA
[c]Department of Neurology, Houston Methodist Hospital, Houston, TX, USA
[d]Department of Psychiatry, University Medicine Greifswald, Greifswald, MV, Germany
[e]Institute for Community Medicine, University Medicine Greifswald, Greifswald, MV, Germany
[f]Department of Neurology, University Medicine Greifswald, Greifswald, MV, Germany
[g]German Center for Neurodegenerative Diseases (DZNE), Rostock/Greifswald, MV, Germany

Abstract

Introduction: We sought to investigate associations of regional white matter hyperintensities (WMHs) within white matter (WM) tracts with cardiovascular risk and brain aging-related atrophy throughout adulthood in the general population, leveraging state of the art pattern analysis methods.
Methods: We analyzed a large sample (n = 2367) from the Study of Health in Pomerania, Germany (range 20–90 years). WMHs were automatically segmented on T1-weighted and fluid-attenuated inversion recovery magnetic resonance images, and WMH volumes were calculated in WM regions defined using the John Hopkins University WM tractography atlas. Regions with the highest average WMH volume were selected. We calculated a subject-specific index, Spatial Pattern of Alteration for Recognition of Brain Aging, to measure age-related atrophy patterns. The Framingham cardiovascular disease risk score summarized the individual cardiovascular risk profile. We used structural equation models, independently for each region, using Spatial Pattern of Alteration for Recognition of Brain Aging as a dependent variable, age as an independent variable, and cardiovascular disease risk score and regional WMH volumes as mediators.
Results: Selected 12 WM regions included 75% of the total WMH burden in average. Structural equation models showed that the age effect on Spatial Pattern of Alteration for Recognition of Brain Aging was mediated by WMHs to a different extent in the superior frontal WM, anterior corona radiata, inferior frontal WM, superior corona radiata, superior longitudinal fasciculus, middle temporal WM, posterior corona radiata, superior parietal WM, splenium of corpus callosum, posterior thalamic radiation, and middle occipital WM (variance explained between 2.8% and 10.3%, $P < .0001$ Bonferroni corrected), but not in precentral WM.
Conclusions: Our results indicate that WMHs, in most WM tracts, might accelerate the brain aging process throughout adulthood in the general population as a result of vascular risk factors, but also independent of them. Preventive strategies against WMHs (such as controlling vascular risk factors or microglia depletion) could delay brain aging.

Keywords: White matter hyperintensities; Alzheimer disease; Brain aging; Cardiovascular disease

The authors declare no competing interests

*Corresponding author. Tel.: +12672887963.
E-mail address: habesm@uphs.upenn.edu

https://doi.org/10.1016/j.dadm.2018.02.002

1. Introduction

Alzheimer's disease accounts for most dementia cases in the general population, followed by vascular dementia. Both dementia types are associated with age and vascular risk factors, which may, in turn, increase the accrual of cerebral white matter hyperintensities (WMHs). WMHs are usually defined by regions of high signal intensity on T2-weighted magnetic resonance (MR) images. WMHs are more prevalent in elderly individuals and are believed to be the result of axonal loss and demyelination that can be triggered by aging, ischemic small vessel disease, and/or neurodegeneration [1–3].

The associations between vascular risk factors and both cerebrovascular pathology and brain aging are well documented [4–6]. Although vascular risk factors could lead to brain aging and cerebrovascular pathology, the resulting overlap remains less quantified in the general population. MR imaging provides a non-invasive way to measure evidence of cerebrovascular disease by quantifying WMH volume so that one can study these complex associations. However, studies reporting the association of specific WMH locations with brain aging and dementia remain scarce [7,8]. In most analyses, WMHs are quantified using a single measure of total burden, or using relatively coarse anatomical parcellations [9], and this might lead to losing sensitivity to location-specific associations of WMHs. Importantly, increasing evidence is pointing to the role of fiber tract-specific WMH burden in neurodegenerative diseases [10,11], the prevalence of which substantially increases with age.

We sought to investigate associations of regional WMHs with cardiovascular risk and brain atrophy patterns related to brain aging throughout adulthood in the general population. We measured regional WMHs from structural MR images, by automatically segmenting and calculating WMH volumes within white matter (WM) tract regions defined on the John Hopkins University WM tractography atlas. We quantified imaging patterns related to aging using a machine learning–based summary index, Spatial Pattern of Alteration for Recognition of Brain Aging (SPARE-BA) [6]. We used structural equation models, independently for each region, for the final analysis.

2. Methods

2.1. Participants from Study of Health in Pomerania

We included in this study 2367 subjects from the Study of Health in Pomerania (SHIP), covering most of the adult life span (range 20–90 years, median = 53 years). SHIP is a population-based prospective cohort, was recruited from the German northern east region of Pomerania, and led by the Institute for Community Medicine at the Medical Faculty of the University of Greifswald [12]. The main focus of SHIP is the investigation of risk factors, preclinical diseases with highly innovative noninvasive methods. The SHIP study covers the human health with all related aspects involving collection and assessment of data. SHIP started at baseline with SHIP-0 between 1997 and 2001. From 2008 to 2013, the second follow-up examination SHIP-2 was carried out. Concurrent with SHIP-2, a new sample from the same area was drawn, and similar examinations were undertaken between 2008 and 2012 (SHIP-Trend). SHIP-2 and SHIP-Trend included whole-body magnetic resonance imaging (MRI) scans and neuroimaging components. The characteristics of this sample is described in Table 1 [1].

In SHIP, 3066 individuals completed both T1-weighted and fluid-attenuated inversion recovery (FLAIR) baseline brain scans. Expert radiologists have visually inspected head MRI scans for artifacts and clinical findings. We excluded in this study scans based on existence of following criteria: clinical stroke, multiple sclerosis, epilepsy, cerebral tumor, intracranial cyst or hydrocephalus (n = 150), and high level of motion artifacts (n = 98) as well as subjects without cognitive testing (n = 176). Further exclusion took place after quality control of the automatically skull-stripped data (n = 121) and the automated WMH segmentation (n = 154). The Ethics Committee of the Medical Faculty of the University of Greifswald approved SHIP.

2.2. Data assessment and laboratory work in SHIP

Clinical data were collected by a computer-assisted face-to-face interview. We divided smoking in three categories, specifically: current smoking, former smoking, and never smoked. Having completed the interview, participants underwent medical examinations, including the measurement of height and weight (continuous variable). Waist circumference was measured in centimeters (continuous variable). After a 5-minute resting period, blood pressure was measured three times on the right arm of seated subjects using a digital blood pressure monitor (HEM-705CP; Omron, Tokyo, Japan), with each reading being followed by a further resting period of 3 minutes. Cuffs were applied according to the circumference of the participant's arm. The mean of the second and third measurements (mm Hg) was used for the analyses (continuous variables). All subjects were informed to bring in their packing containers of all medication they had taken during the last 7 days, as well as their drug prescription sheets. Every compound was recorded. We used antihypertensive, antidiabetic, and lipid-lowering drugs, as indicators for cardiovascular disease (CVD) risk factors in the general population. High-density lipoprotein cholesterol concentrations were measured photometrically (Hitachi 704; Roche, Mannheim, Germany). Total cholesterol, low-density lipoprotein, and high-density lipoprotein were measured as dimensional scores.

2.3. Image acquisition

SHIP included whole-body MRI protocol [13]. The neurocranium module of SHIP included, among others,

Table 1
Description of the SHIP sample included in this study

Characteristic	SHIP subcohort		
	SHIP-2 (n = 730)	SHIP-Trend (n = 1637)	SHIP study sample (n = 2367)
Age, mean (SD), years	55.60 (12.30)	51.00 (14.06)	52.42 (13.71)
Gender, N (%), female	399 (54.60)	920 (56.20)	1319 (56.72)
Systolic blood pressure, mean (SD), mm Hg	131.20 (17.98)	125.54 (17.11)	127.29 (17.58)
Total cholesterol, mean (SD), mmol L^{-1}	5.51 (1.07)	5.53 (1.07)	5.52 (1.07)
High-density lipoprotein, mean (SD), mmol L^{-1}	1.46 (0.38)	1.46 (0.37)	1.46 (0.37)
Low-density lipoprotein, mean (SD), mmol L^{-1}	3.35 (0.93)	3.42 (0.92)	3.40 (0.92)
Waist circumference, mean (SD), cm	89.77 (12.75)	88.70 (12.80)	89.03 (12.79)
Education, N (%)			
<8 years	135 (18.49)	234 (14.29)	369 (15.58)
8–10 years	420 (57.53)	900 (54.97)	1320 (55.76)
>10 years	175 (25.97)	503 (30.72)	678 (28.64)
Cigarette smoking, N (%)			
Never smoker	291 (39.86)	676 (41.29)	967 (40.85)
Ex-smoker	300 (41.09)	577 (35.24)	877 (37.05)
Current smoker	139 (19.04)	384 (23.45)	523 (22.09)
Medication			
Antidiabetics, N (%)	38 (5.20)	62 (3.78)	100 (4.22)
Antihypertensive, N (%)	269 (36.84)	504 (30.78)	773 (32.65)
Lipid lowering drugs, N (%)	116 (15.89)	137 (8.36)	253 (10.68)

Abbreviations: SD, standard deviation; SHIP, Study of Health in Pomerania.
Modified from [1].

T1-weighted and FLAIR sequences. In SHIP, the same 1.5-T Siemens MRI scanner (Magnetom Avanto; Siemens Medical Systems, Erlangen, Germany) was used for all subjects. The T1-weighted image was acquired with the following parameters: 1 × 1 mm in-plane spatial resolution, 1.0-mm slice thickness (flip angle 15°), 3.4-ms echo time, and 1900-ms repetition time. The T2 FLAIR images were acquired using the following parameters: 0.9 × 0.9 mm in-plane spatial resolution, 3.0-mm slice thickness (flip angle 15°), 325-ms echo time, and 5000-ms repetition time.

2.4. WMH quantification

We delineated WMHs by applying a supervised learning-based multimodal segmentation algorithm on the FLAIR and T1 scans of subjects [1]. The John Hopkins University atlas image [14] was aligned into each subject's T1-weighted image using deformable registration, to transfer atlas labels to subject image space. WMH volumes within each region of interest were calculated and were normalized by the total intracranial volume of the subject.

2.5. Calculation of the SPARE-BA index

Using a high-dimensional pattern analysis method, we calculated an index, named as SPARE-BA as described previously [6]. This index summarizes age-related brain atrophy patterns of an individual with a single value, using as input volumetric image features normalized by intracranial volume. SPARE-BA methodology relies on a linear support vector machine–based model to learn atrophy patterns that can optimally discriminate old versus relatively younger subjects with structural imaging data. Lower values of the SPARE-BA index indicated presence of more aging-related atrophy patterns and vice versa. SPARE-BA patterns were capturing mostly gray matter decrease in insular cortex, thalamus, cingulate, frontal, inferior parietal, and lateral temporal cortex [6]. We calculated individual SPARE-BA scores for SHIP subjects through 10-fold cross-validation.

2.6. Vascular risk factors

A modified version of the Framingham CVD risk score (CVD-RS) was used to summarize a set of risk factors, that is, gender, total cholesterol level, high-density lipoprotein, systolic blood pressure, systolic blood pressure treatment status, diabetes mellitus, and smoking, via a single score reflecting the individual cardiovascular risk profile [15]. We did not include age in this risk score, to investigate associations between vascular risk factors other than the age with aging-related brain atrophy.

2.7. Statistical analyses

To investigate the contributions of CVD-RS and regional WMH volume on brain aging, both jointly and independently, we used structural equation modeling implemented in the lavaan package (https://cran.r-project.org/web/packages/lavaan/index.html) [16]. We constructed one independent model for each regional WMH measurement, where we modeled the SPARE-BA index as a dependent variable, age as an independent variable, and CVD-RS and regional WMH volume as mediators. Subsequent analyses and graphics were done using R software (v3.0) [17].

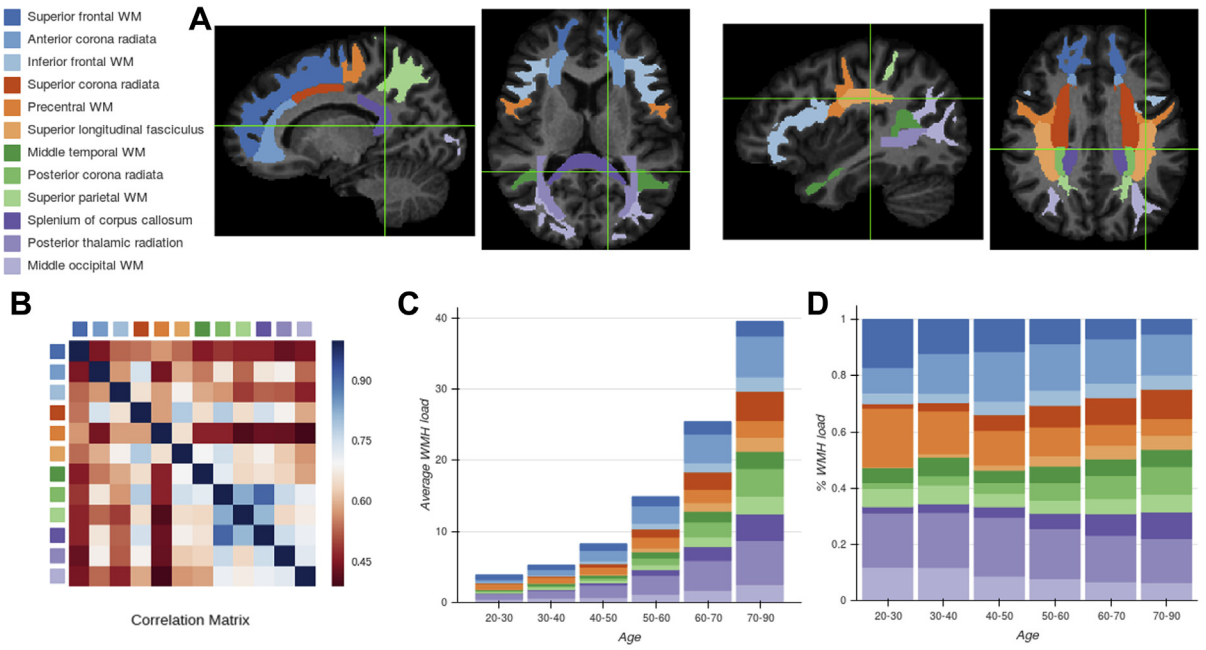

Fig. 1. Tract-specific distribution of WMHs in the SHIP cohort. (A) Axial and sagittal views of the 12 regions of interest from the JHU WM tractography atlas, which were selected based on having the highest average WMH volume in the SHIP cohort (75% of the total WMH load included within the selected regions). Please note that the ordering of the regions is not based on average WMH volumes, but on their anatomical location, with a sorting from anterior to posterior. (B) The correlation matrix of the pairwise correlations for the WMH volumes of region pairs. (C) Average regional WMH volumes for subjects in each decade of age. (D) Percent regional WMH volumes (regional volumes were normalized by the total WMH volume in all selected regions) for subjects in each decade of age. Abbreviations: JHU, John Hopkins University; SHIP, Study of Health in Pomerania; WM, white matter; WMH, white matter hyperintensity.

3. Results

In the tract-based parcellation of WMHs (Fig. 1A), the 12 regions with the highest average WMH burden included 75% of all WMH volume overall. WMH volume increased exponentially with age (Fig. 1C–D). Regional WMH volumes within selected WM tracts were very highly correlated between each other (Fig. 1B). Nonetheless, regional WMH volumes also showed subtle differentiations in their age trends, particularly with a slower rate of increase in relative WMH volumes in frontal regions, compared to more posterior regions (Fig. 1D). The SPARE-BA model achieved a high predictive accuracy (Pearson's correlation $r = -0.803$ between the actual and predicted ages, with 10-fold cross-validation), indicating that it was successful in capturing age-related brain atrophy patterns with a single summary index value.

Structural equation modeling showed that the age effect on brain aging patterns captured by the SPARE-BA score was partly mediated by WMH volume in all regions with a differential involvement (variance explained between 2.8% and 10.3%, $P < .0001$ Bonferroni corrected), except in the precentral WM ($P = .102$; Fig. 2). Also, the effect of age on SPARE-BA was mediated by CVD-RS (through the paths d-e and c-d-b in Fig. 2) in all models (variance explained 6.1%, $P < .05$ Bonferroni corrected). The cardiovascular risk score was associated with WMHs (path c in Fig. 2) in all regions ($P < .0001$ Bonferroni corrected). The strongest effect of age was the direct one (variance explained between 84.1% and 93.0%, $P < .0001$). Supplementary analysis with coarser anatomically defined regions, frontal, parietal-temporal, and occipital lobes yielded similar results (Supplementary Materials).

4. Discussion

In a large sample (n = 2367) from the general population (SHIP), we showed that WMHs might accelerate the brain aging process throughout adulthood as a result of major vascular risk factors, but also independent of them. To our knowledge, this is one of the few reports investigating contributions of regional WMHs within WM tracts to advanced brain aging and their mediation on age effects together with vascular risk factors using structural equation modeling.

MR image analyses in this study were performed using advanced techniques to automatically segment WMHs, to measure WMH load within automatically delineated regions of interest predefined on a WM tractography atlas, and to quantify brain aging by applying a high-dimensional pattern classification method. In our structural equation models, we used the SPARE-BA index as the dependent variable. This imaging index, which summarizes multivariate regional atrophy patterns associated with aging via a single value, was essential in our models for capturing advanced brain aging patterns, that is, those beyond atrophy patterns seen in

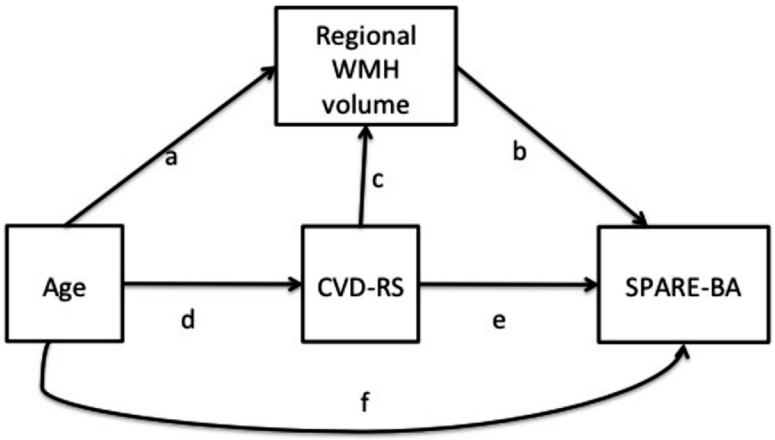

Weights of structural equation models

Region of interest	a-b	d-c-b	d-e	f	a-b and d-c-b (for WMH)
Superior frontal WM	2.43**	0.33*	5.78**	91.46**	2.76**
Anterior corona radiata	9.63**	0.68*	5.43**	84.26**	10.31**
Inferior frontal WM	3.86**	0.52*	5.59**	90.03**	4.38**
Superior corona radiata	5.84**	0.44*	5.67**	88.05**	6.28**
Precentral WM	1.08	0.19	5.92**	92.81**	1.27
Superior longitudinal fasciculus	2.82**	0.32*	5.79**	91.07**	3.14**
Middle temporal WM	3.89**	0.64*	5.47**	90.00**	4.53**
Posterior corona radiata	5.39**	0.39*	5.72**	88.50**	5.78**
Superior parietal WM	4.18**	0.36*	5.75**	89.70**	4.55**
Splenium of corpus callosum	7.59**	0.56*	5.55**	86.29**	8.16**
Posterior thalamic radiation	9.76**	0.53*	5.58**	84.13**	10.28**
Middle occipital WM	5.90**	0.43*	5.68**	87.99**	6.33**

Fig. 2. Structural equation models showing potential causal associations of tract-specific white matter hyperintensities in the selected regions, with brain aging patterns of atrophy (SPARE-BA) across the adulthood life span from the SHIP sample (range 20–90 years, median = 53 years). The path diagram of the 12 models (top); calculated estimates for relevant paths leading to more brain aging patterns (bottom). ** significant at $P < .0001$ and * significant at $P < .05$. Abbreviations: CVD-RS, cardiovascular disease risk score; SPARE-BA, Spatial Pattern of Alteration for Recognition of Brain Aging; SHIP, Study of Health in Pomerania; WMH, white matter hyperintensity.

normal aging, and for investigating links to WMHs and CVD.

4.1. Age trends of WMHs

Our work extends previous reports that demonstrated an age-related increase in WMHs [2,7], by investigating regional associations of WMHs in WM tract regions. We observed that WMH volume in each region of interest increased with age. Importantly, age-related changes in WMH burden showed differences between regions, with higher volume and percentage of WMHs in the frontal areas until middle age, while in older ages, we observed higher WMH volume and percentage of burden in parietal-temporal regions. The increase in percentage in parietal-temporal regions might be linked to increase in prevalence of neurodegeneration in elderly.

The importance of tract-specific analysis for understanding their effect on brain function was acknowledged; however, large aging cohort studies remain limited [9].

Our study recruited 2367 scans from a general population sample, making it one of the largest studies so far that maps WMHs into WM tract-specific regions. The fact that WMHs involve damage to projection fiber tracts could explain their link to deficits in specific brain structures and, ultimately, to function. For example, we found age-related increase in WMHs in the inferior frontal WM, in the superior frontal WM, and in anterior corona radiata. Frontal WMHs might affect tracts in the prefrontal cortex resulting in decreases in the prefrontal cortex activity, in addition to medial temporal and anterior cingulate regions [18]. Age-related WMHs could affect tracts that are involved in processing speed (superior corona radiata) and movement (precentral WM) and thus give insights on age-related impairment in those functions.

WMHs are often considered a reflection of small vessel disease, and accordingly they are associated with vascular risk factors. Our data confirmed this link for frontal, parietal-temporal, and occipital WMHs. It has been suggested that vascular risk factors lead to structural brain changes in the aging brain via cerebrovascular disease, for which WMHs are a hallmark [19], together with gray matter atrophy [4]. Our data support vascular and nonvascular age-related WMH changes, as WMHs and vascular risk factors were associated with SPARE-BA patterns with an overlapping path, but also independently. These results through vascular pathways are not surprising as even different vascular risk factors are associated with specific brain vulnerability. For example, a previous report from the SHIP cohort showed widespread brain atrophy associated with obesity [20], while hypertension might lead to small vessel disease and higher WMH burden [5]. On the other hand genetic predisposition, specifically myelin genes, may (partly) explain the non-vascular factors leading to WMHs and subsequently age-related brain atrophy [21].

4.2. Associations of regional WMHs and aging-related brain atrophy

We have found significant associations between WMH volume in WM tract regions and aging-related brain atrophy patterns, albeit without differences in region-specific significance. The lack of region-specific significance can be due to a variety of reasons. Most importantly, the high correlation between WMH load in different frontal and parietal-temporal regions may suggest a general widespread deterioration of the WM with aging. Regional WMH change might be better captured with more specific aspects of brain aging rather than a global measure such as SPARE-BA.

Nevertheless, WMHs within the anterior corona radiata had the largest proportion (10.3%) of mediating the age effect on aging-related atrophy. This could be explained by chronic hypoperfusion in the watershed distribution area between the middle cerebral artery and the anterior cerebral artery.

4.3. Strengths and limitations

This study has several strengths including the large sample size from the general population, with a fully standardized protocol and the same scanner for brain imaging, but also it suffers from some limitations. We did not incorporate other measures of small vessel disease like microbleeds or lacunes. Furthermore, this is a cross-sectional study and a longitudinal assessment of the relationship between these measures and cognitive change would increase understanding of the temporal course of these effects. Finally, in this study, we used the Framingham formula to assess individual's cardiovascular risk profile for a German population; however, other formulas also exist such as the clinically wide used American Heart Association pooled equation in the United States or the Joint British Societies risk score in Britain. Although the debate in the literature continues for the "optimal" risk score in a given population [22], other risk scores rather than the Framingham formula should be also considered in future research.

5. Conclusion

Our results indicate that, in most WM tracts, WMHs might accelerate the brain aging process throughout adulthood in the general population as a result of vascular risk factors, but also independent of them. Preventive strategies against WMHs (such as controlling vascular risk factors or microglia depletion [21]), might delay brain aging. Potential prevention and treatment strategies could be evaluated and monitored using quantitative MRI analysis.

Acknowledgments

SHIP is part of the Community Medicine Research net of the University of Greifswald, Germany, which is funded by the Federal Ministry of Education and Research (grants no. 01ZZ9603, 01ZZ0103, and 01ZZ0403), the Ministry of Cultural Affairs, and the Social Ministry of the Federal State of Mecklenburg-West Pomerania. Genome-wide data in SHIP and MRI scans in SHIP and SHIP-TREND have been supported by a joint grant from Siemens Healthcare, Erlangen, Germany, and the Federal State of Mecklenburg-West Pomerania. Genome-wide genotyping in SHIP-TREND-0 was supported by the Federal Ministry of Education and Research (grant no. 03ZIK012). This work has been supported in part by The Allen H. and Selma W. Berkman Charitable Trust (Accelerating Research on Vascular Dementia) and NIH (grant no. 1RF1AG054409).

Supplementary data

Supplementary data related to this article can be found at https://doi.org/10.1016/j.dadm.2018.02.002.

RESEARCH IN CONTEXT

1. Systematic review: We searched PubMed using the terms: "Regional" or "frontal" or "temporal" or "parietal" or "occipital" or "fornix," "tract-specific," "white matter hyperintensities," "WMH," "white matter lesions," "WML," and "Brain Aging", "Alzheimer's disease," or "dementia."
2. Interpretation: Our results indicate that most of tract-specific white matter hyperintensities (WMHs) might accelerate the brain aging process throughout adulthood in the general population as a result of vascular risk factors, but also independent of them. Identifying etiologies leading to WMHs could lead to preventive strategies against WMHs, which could help to delay brain aging, and treatment response could be monitored using MRI biomarker measurements.
3. Future directions: Continued follow-up of our analysis in further cohorts with longitudinal data will allow us to perform a longitudinal assessment of the relationship between regional WMHs and cognitive change and would increase understanding of the temporal course of their effects.

References

[1] Habes M, Erus G, Toledo JB, Zhang T, Bryan N, Laune LJ, et al. White matter hyperintensities and imaging patterns of brain aging in the general population. Brain 2016;139(Pt 4):1164–79.

[2] Prins ND, Scheltens P. White matter hyperintensities, cognitive impairment and dementia: an update. Nat Rev Neurol 2015;11:157–65.

[3] Wardlaw JM, Valdés Hernández MC, Muñoz-Maniega S. What are white matter hyperintensities made of? Relevance to vascular cognitive impairment. J Am Heart Assoc 2015;4:001140.

[4] Debette S, Seshadri S, Beiser A, Au R, Himali J, Palumbo C, et al. Midlife vascular risk factor exposure accelerates structural brain aging and cognitive decline. Neurology 2011;77:461–8.

[5] Wardlaw JM, Smith C, Dichgans M. Mechanisms of sporadic cerebral small vessel disease: insights from neuroimaging. Lancet Neurol 2013;12:483–97.

[6] Habes M, Janowitz D, Erus G, Toledo J, Resnick SM, Doshi J, et al. Advanced Brain Aging: relationship with epidemiologic and genetic risk factors, and overlap with Alzheimer disease atrophy patterns. Transl Psychiatry 2016;6:e775.

[7] Kim JH, Hwang KJ, Kim JH, Lee YH, Rhee HY, Park K-C. Regional white matter hyperintensities in normal aging, single domain amnestic mild cognitive impairment, and mild Alzheimer's disease. J Clin Neurosci 2011;18:1101–6.

[8] Brickman AM, Provenzano FA, Muraskin J, Manly JJ, Blum S, Apa Z, et al. Regional white matter hyperintensity volume, not hippocampal atrophy, predicts incident Alzheimer disease in the community. Arch Neurol 2012;69:1621–7.

[9] Biesbroek JM, Weaver NA, Biessels GJ. Lesion location and cognitive impact of cerebral small vessel disease. Clin Sci (Lond) 2017;131:715–28.

[10] Taylor ANW, Kambeitz-Ilankovic L, Gesierich B, Simon-Vermot L, Franzmeier N, Araque Caballero MA, et al. Tract-specific white matter hyperintensities disrupt neural network function in Alzheimer's disease. Alzheimers Dement 2017;13:225–35.

[11] Kantarci K, Murray ME, Schwarz CG, Reid RI, Przybelski SA, Lesnick T, et al. White-matter integrity on DTI and the pathologic staging of Alzheimer's disease. Neurobiol Aging 2017;56:172–9.

[12] Völzke H, Alte D, Schmidt CO, Radke D, Lorbeer R, Friedrich N, et al. Cohort Profile: The Study of Health in Pomerania. Int J Epidemiol 2011;40:294–307.

[13] Hegenscheid K, Kühn JP, Völzke H, Biffar R, Hosten N, Puls R. Whole-body magnetic resonance imaging of healthy volunteers: pilot study results from the population-based SHIP study. Rofo 2009;181:748–59.

[14] Mori S, Wakana S, Van Zijl PC, Nagae-Poetscher L. MRI Atlas of Human White Matter. Amsterdam: Elsevier; 2005.

[15] D'Agostino RB, Vasan RS, Pencina MJ, Wolf PA, Cobain M, Massaro JM, et al. General cardiovascular risk profile for use in primary care: The Framingham Heart Study. Circulation 2008;117:743–53.

[16] Rosseel Y. lavaan: An R package for structural equation modeling. J Stat Softw 2012;48:1–36.

[17] Team RDC. R: A Language and Environment for Statistical Computing. Vienna, Austria: R Foundation for Statistical Computing; 2008.

[18] Nordahl CW, Ranganath C, Yonelinas AP, Decarli C, Fletcher E, Jagust WJ. White matter changes compromise prefrontal cortex function in healthy elderly individuals. J Cogn Neurosci 2006;18:418–29.

[19] Gorelick PB. Risk factors for vascular dementia and Alzheimer disease. Stroke J Cereb Circ 2004;35:2620–2.

[20] Janowitz D, Wittfeld K, Terock J, Freyberger HJ, Hegenscheid K, Völzke H, et al. Association between waist circumference and gray matter volume in 2344 individuals from two adult community-based samples. Neuroimage 2015;122:149–57.

[21] Janova H, Arinrad S, Balmuth E, Mitjans M, Hertel J, Habes M, et al. Microglia ablation alleviates myelin-associated catatonic signs in mice. J Clin Invest 2017;128:734–45.

[22] Guerra-Silva NM, Santucci FS, Moreira RC, Massao Tashima C, de Melo SC, Pereira LR, et al. Coronary disease risk assessment in men: comparison between ASCVD Risk versus Framingham. Int J Cardiol 2017;228:481–7.